

# Effect of solar radiation and temporal variations on forest fire occurrence and severity in the Ethiopian highlands

Ammanuel Hailye, Yanchuang Zhao\*, Xingdong Wang, Hongjun Zha, Yuhua Wang

College of Information Science and Engineering, Henan University of Technology, Zhengzhou 45001, China

---

**Abstract:** Solar radiation and temporal climatic variations are widely recognized as key drivers in the occurrence and spread of forest fires across the globe, with particularly pronounced impacts in ecologically sensitive regions such as the Ethiopian Highlands. This study investigates the role of solar radiation in influencing forest fire activity by exploring the correlation between Land Surface Temperature (LST) and observed fire events. Utilizing satellite-derived thermal datasets in conjunction with fire occurrence and severity data, this study aims to uncover spatiotemporal patterns that reveal how elevated temperature regimes contribute to the ignition, intensity, and progression of forest fires in the region. A correlational analytical framework is employed to assess the relationship between LST and fire severity metrics, notably the differenced Normalized Burn Ratio (dNBR). By quantifying these relationships, the study enhances understanding of the thermal dynamics underlying fire behavior. The findings are expected to support the development of predictive fire risk models and to inform evidence-based fire management strategies. Furthermore, the insights contribute to ongoing discourse on climate change adaptation, particularly in highland ecosystems vulnerable to increasing thermal stress and environmental degradation.

**Keywords:** Forest fires, Ethiopian Highlands, Remote sensing, Satellite imagery, LST, dNBR

---

Date of Submission: 13-04-2025

Date of acceptance: 28-04-2025

---

## I. Introduction

Remote sensing technologies have revolutionized forest fire detection by enabling efficient monitoring of large and inaccessible areas through the integration of Land Surface Temperature (LST) data and spectral indices such as the Normalized Burn Ratio (NBR) and the differenced Normalized Burn Ratio (dNBR). These tools allow for timely identification of active fires, assessment of burn severity, and improved understanding of fire dynamics across diverse landscapes. The East Benishangul-Gumuz Wildlife Protection Park is located in the northwestern region of Ethiopia. Spanning an area of approximately 50,381 square kilometers, this vast ecological landscape is situated at altitudes ranging from 1,200 to 1,500 meters above sea level. The region experiences annual temperatures fluctuating between 20°C and 40°C. Geographically, the park lies between 9°17' to 12°06' North latitude and 34°04' to 37°04' East longitude. It encompasses a wide array of ecosystems and harbors rich biodiversity, including various vegetation types and wildlife species (Fig. 1). Climate variability plays a significant role in shaping fire regimes, particularly in ecologically sensitive and topographically complex regions such as the Ethiopian highlands. Among the various climatic drivers, solar radiation and its influence on land surface temperature (LST) are central to understanding vegetation flammability and fire susceptibility. In regions with pronounced dry seasons, increased solar radiation leads to reduced vegetation moisture, drying of ground fuel, and overall elevated fire risk. Temporal variations, including shifts in seasonal weather patterns and inter-annual climate anomalies, further exacerbate these risks by altering the frequency, duration, and intensity of fire-prone conditions. While these dynamics have been extensively studied in Mediterranean and temperate ecosystems, their specific impacts in high-altitude tropical regions like the Ethiopian Highlands remain understudied.

Several remote sensing-based studies have explored the linkage between LST and wildfire activity. Gitas et al. (2012) emphasized the importance of incorporating thermal indicators into fire risk models, particularly in areas with limited ground-based data [1]. Chuvieco et al. (2006) demonstrated that satellite-derived thermal anomalies can act as reliable early warning indicators for fire outbreaks when combined with vegetation indices and historical fire data [2]. These findings are supported by other research efforts, including Veraverbeke et al. (2014) and Sun et al. (2019), which confirmed that integrating thermal data with post-fire indices such as the differenced Normalized Burn Ratio (dNBR) enhances the accuracy of burn severity assessments across diverse landscapes. Despite these advances, a major gap remains in applying these

techniques to African highland ecosystems, which exhibit distinct climatic, ecological, and topographic characteristics [3][4].

The Ethiopian highlands, encompassing large swaths of forest, grassland, and agricultural mosaics, experience significant variations in elevation, land cover, and solar exposure. These factors influence microclimates and fuel conditions, making standard fire detection and assessment models less reliable without regional calibration. Most existing models rely on thresholds and algorithms developed for temperate or semi-arid environments and often fail to capture the nuanced behavior of fire in high-altitude, mixed-vegetation systems. For example, the dNBR index, while widely used globally, requires contextual adaptation to effectively reflect burn severity in this region. Miller et al. (2009) and Bastarrika et al. (2011) both highlighted the importance of adjusting dNBR thresholds according to local biophysical variables to reduce errors in fire mapping and classification [5][6].

One particularly promising approach involves the integration of LST with terrain and temporal variables to produce a more holistic fire risk model. Studies conducted in varied geographic regions suggest that pre-fire LST anomalies, especially when sustained over dry periods, can signal increased ignition potential. In mountainous or highland regions, however, topographic factors such as slope, elevation, and aspect further influence solar radiation exposure and, by extension, the spatial variability of LST. Incorporating these variables into fire detection and severity models is especially crucial for the Ethiopian highlands, where terrain plays a pivotal role in shaping microclimates and vegetation distribution.

This study aims to fill the existing research gap by examining the relationship between solar radiation represented by satellite-derived LST and forest fire dynamics in East Benishangul-Gumuz Wildlife Protection Park. By correlating LST with fire occurrence and severity (measured via dNBR). Furthermore, the inclusion of seasonal patterns allows for the analysis of temporal variation in fire behavior, offering insights into how different climatic periods influence ignition and burn severity. The outcomes of this study have the potential to refine fire monitoring strategies in Ethiopia and contribute to the global understanding of fire ecology in highland environments facing increasing climate variability.

## II. Data and Methods

### 2.1 Principles and methods

This study employed the Land Surface Temperature (LST) that derived from the thermal infrared (TIR) bands of Landsat 8, specifically Band 10 or Band 11. The calculation of LST involves multiple steps, which will be systematically outlined in the following sections to ensure accurate results. The steps are shown below in Fig 2.

#### Top-of-Atmosphere (TOA) Radiance

Top-of-Atmosphere (TOA) Radiance refers to, the amount of radiative energy received by a satellite sensor per unit area, per unit solid angle, and per unit wavelength at the top of Earth's atmosphere [7][8]. It represents the raw radiance values detected by the satellite before any atmospheric corrections are applied. To calculate this value, we must gather the digital number (DN) of the pixel from the metadata. Then the formula to calculate TOA is as follows:

$$L_{\lambda} = M_L * DN + A_L \quad (1)$$

where:  $M_L$  is radiance multiplicative scaling factor (from metadata)

$A_L$  is radiance additive scaling factor (from metadata)

DN is digital number of the pixel

Landsat's thermal bands (TIRS) provide digital numbers (DNs) that must be converted to radiance ( $L_{\lambda}$ ). After we acquire the radiance conversion factors from Landsat 8 Band 10, we calculate the radiance.

#### Brightness Temperature (BT)

Brightness Temperature (BT) is the temperature of a blackbody that would emit the same amount of radiance as detected by a satellite sensor in a specific thermal infrared (TIR) band. It approximates the actual surface temperature but is influenced by atmospheric effects, surface emissivity, and sensor calibration [9]. Once we have the radiance, we use Planck's equation to get the brightness temperature (BT). The formula is as follows:

$$BT = \frac{K_2}{\ln\left(\frac{K_1}{L} + 1\right)} \quad (2)$$

where: BT is Brightness temperature in Kelvin,

L is TOA radiance

$K_1, K_2$ = Sensor-specific thermal calibration constants. Landsat 8 band 10 ( $K_1= 774.8853$  and  $K_2= 1321.0789$ ).

#### Land Surface Temperature (LST)

LST is the efficiency of a surface in emitting thermal radiation relative to a perfect blackbody. Ranges from 0 to 1, water (~0.99) has high emissivity, and bare soil (~0.85–0.95) has lower emissivity [10]. We need LST

correction because Brightness Temperature (BT) from satellites assumes a blackbody surface, which can cause temperature overestimation or underestimation. We can calculate by using the following equation:

$$LST = \frac{BT}{1 + \left(\frac{\lambda}{c_2}\right) \ln \varepsilon} \quad (3)$$

where:  $\lambda$  is Wavelength of thermal radiation (10.9  $\mu\text{m}$  for Landsat 8 band 10)

$c_2$  is  $1.438 \times 10^{-2}$  mK (second Planck constant)

$\varepsilon$  is Land surface emissivity (depends on land cover type)

BT is Brightness temperature

By applying these methods, we can derive accurate thermal remote sensing products essential for environmental and scientific analyses [11].

### **differenced Normalized Burn Ratio (dNBR)**

This study employed the differenced Normalized Burn Ratio (dNBR) index to extract fire-affected areas through spectral analysis of satellite imagery before and after fire events. dNBR leverages the spectral reflectance in the Near-Infrared (Band 5) and Short-Wave Infrared (Band 7) to quantify burn severity [12]. For this method, the Normalized Burn Ratio (NBR) is calculated independently for pre-fire and post-fire images using the formula:

$$NBR = \frac{\text{Band 5} - \text{Band 7}}{\text{Band 5} + \text{Band 7}} \quad (4)$$

The differenced Normalized Burn Ratio (dNBR) is calculated by subtracting the post-fire NBR from the pre-fire NBR. This yields positive values for burned areas, with higher values indicating greater burn severity, while unburned areas typically produce values close to zero or negative. [13].

### **2.2 Data collection process**

This study utilized satellite data from Landsat 8 OLI\_TIRS. All datasets were acquired from the United States Geological Survey (USGS) through the Earth Explorer platform. Landsat 8 imagery covering the period from 2024 to 2024 was selected for the study area, corresponding to WRS-2 path/row 170/53. To capture seasonal variability, both pre-fire (wet season) and post-fire (dry season) images were collected. Upon acquisition, the remote sensing data underwent preprocessing procedures, including atmospheric correction, radiometric calibration, and geometric correction, to ensure consistency and accuracy for subsequent analysis. The locations of the study regions are illustrated in Fig. 1

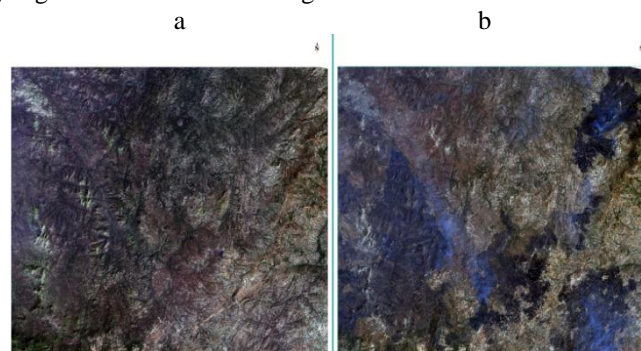


**Fig.1** Study regions (a)pre-fire, (b)post fire

### **Variation of annual temporal data**

Fires in the Ethiopian highlands are more frequent during the dry season due to lower moisture levels in vegetation and soil. Seasonal analysis helps identify periods of heightened fire risk, enabling targeted interventions. For temperature analysis, we focus on maximum temperature records to assess fire risk. This section examines the relationship between seasonal temperature variations and fire severity by comparing historical temperature data with detected burned areas. Higher temperatures during the dry season typically increase fire severity. We analyze forest fire distribution in the Chagni area from 2016 to 2024, focusing on dry (January–May) and wet (June–November) seasons. Peak temperatures, occurring between March and May, coincide with the dry season, when fire frequency and severity are highest due to extreme dryness. In contrast, the lowest temperatures are observed between July and September, aligning with the wet season, when increased rainfall and cloud cover reduce fire risk. Temperature fluctuations range from 27°C to 40°C, with recurring seasonal patterns.

The main workflow for acquisition of Land Surface temperature (LST) data are shown in Fig. 2.

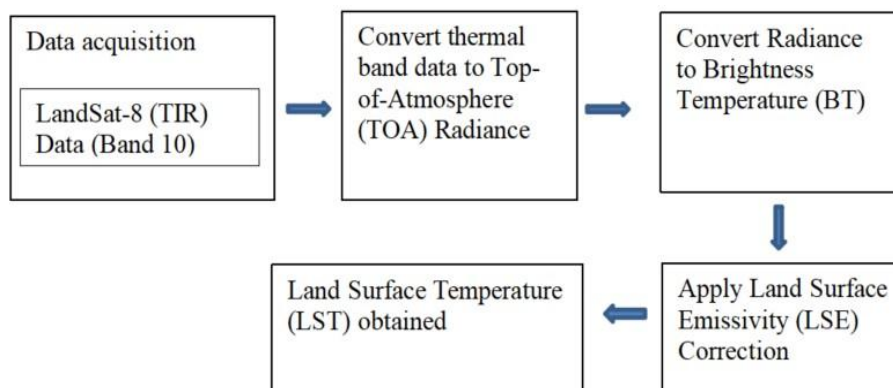


**Fig. 2** Acquisition process of LST data

### III. Data processing

#### 3.1 LST data processing

To obtain the Land Surface Temperature (LST), we process the Top-of-Atmosphere (TOA) Radiance represents the raw radiative energy received by the satellite sensor before atmospheric corrections. Then, Brightness Temperature (BT) provides an estimate of the temperature of an equivalent blackbody emitting the same radiance observed in a specific thermal infrared (TIR) band. However, since real-world surfaces have varying emissivity, this estimate can be inaccurate. To refine the measurement, Land Surface Temperature (LST) is calculated by correcting BT for surface emissivity variations, producing a more precise representation of actual surface temperatures. By following these steps, we obtain a corrected, reliable estimation of Earth's surface temperature, essential for our temperature effect on forest fire study.

We calculated the Land Surface Temperature (LST), and we changed the map into a color-coded heatmap for enhanced visualization and assessment. The results are shown below.

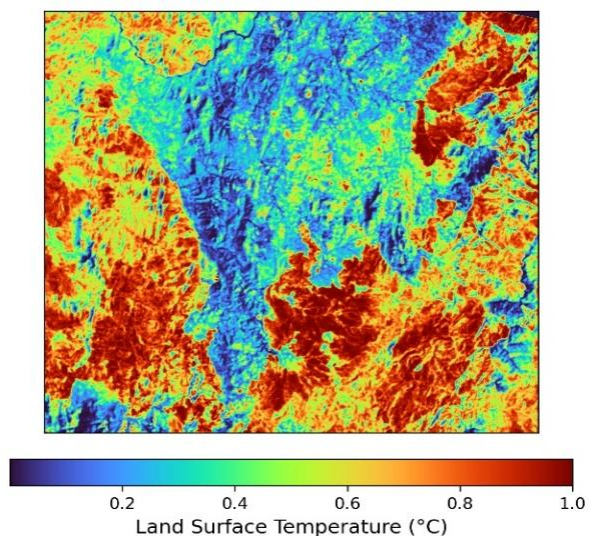


**Fig. 3** Land Surface Temperature (LST) of the study area, scaled 0 to 1, lowest to highest

#### 3.2 dNBR image processing

For Landsat 8, the Normalized Burn Ratio (NBR) is calculated using band 5 (0.85-0.88  $\mu\text{m}$ ) and band 7 (2.11-2.29  $\mu\text{m}$ ). NBR is calculated as:  $(\text{Band5} - \text{Band7}) / (\text{Band5} + \text{Band7})$ . The values before the fire range from 0.22 to 0.58. These values are generally positive, indicating unburned vegetation. NBR values after the fire range from -0.28 to 0.50. Areas with negative values typically indicate burned regions. Then next, we calculate the dNBR value by subtracting the post-fire NBR from the pre-fire NBR. Burned areas appear brighter than the surrounding areas. The resulting range of the dNBR values is -0.23 to 0.57. The result is shown in Fig. 4

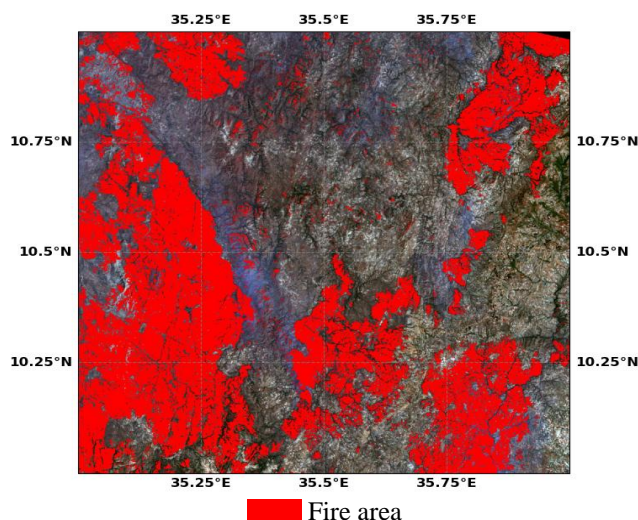


Fig.4 dNBR image of the study area

#### IV. Correlation

##### 4.1 Pearson correlation between dNBR and LST

The relationship between Differenced Normalized Burn Ratio (dNBR) and Land Surface Temperature (LST) is crucial in understanding fire severity and post-fire landscape recovery. dNBR is a widely used remote sensing index that quantifies fire-induced vegetation changes by analyzing pre- and post-fire near-infrared and shortwave infrared reflectance. LST, derived from thermal infrared satellite data, represents the Earth's surface temperature and can be an indicator of fire intensity and residual heat. By conducting a correlation analysis between dNBR and LST, we can assess whether higher burn severity (higher dNBR values) corresponds to increased surface temperatures, which can provide insights into fire behavior, energy release, and ecological impacts. This study aims to explore the strength and significance of this relationship, helping to refine fire impact assessments and improve fire severity classification models. Fig. 5 shows correlation analysis between dNBR and LST.

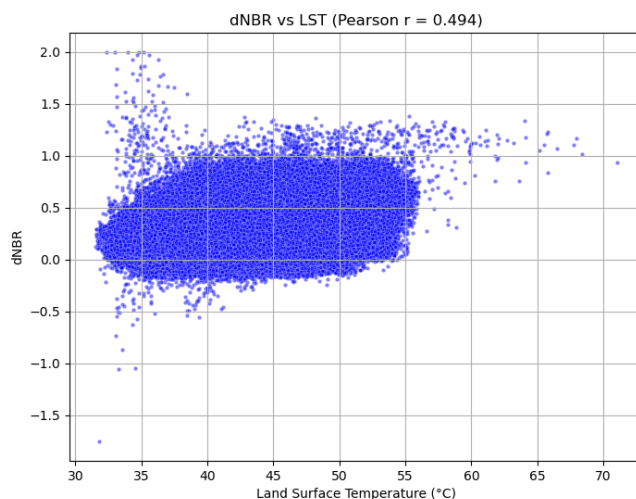


Fig. 5 Correlation analysis between dNBR and LST

The Pearson correlation coefficient ( $r = 0.494$ ) indicates a moderate positive relationship between Land Surface Temperature (LST) and the differenced Normalized Burn Ratio (dNBR). This suggests that areas with higher surface temperatures tend to have higher burn severity, but the relationship is not strong, meaning other factors also influence fire severity. This could be vegetation type burn differently, impacting dNBR also terrain and aspect slopes and orientations affect fire spread and heat retention. Moreover, pre-fire conditions like moisture content, fuel load, and wind conditions could influence burn severity. Therefore, we must continue the analysis using more data inputs.

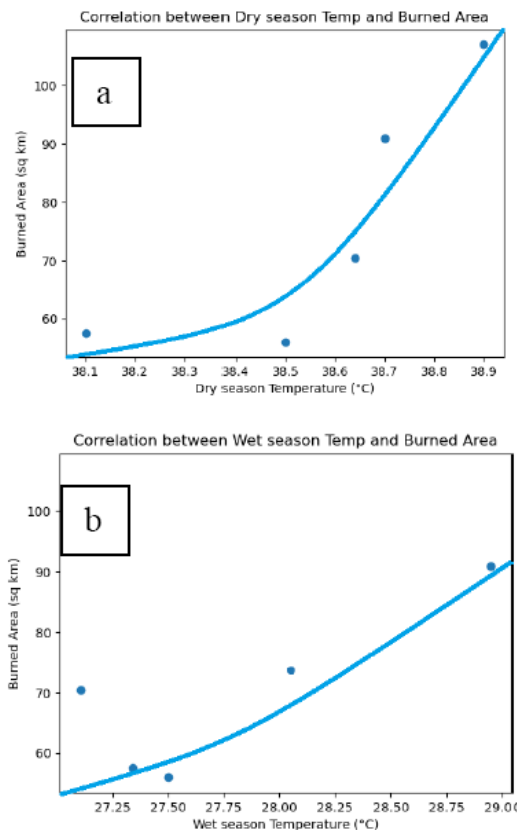
#### 4.2 Pearson correlation between fire area and seasonal tempratures

In the 6 years of 2016-2022, the highest peak temperature was recorded in the dry season. At the same time, the results from threshold value and burned area calculation of each year interval of 8-year periods are also obtained, as shown in Table 5-1. It presents a summary of fire-related metrics and temperature trends across five different periods between 2016 and 2024. It includes the fire-affected area calculated in hectares, and corresponding temperature data. The annual high temperatures remain relatively consistent, ranging from 39.16°C to 39.97°C. The dry season hot temperatures show slight fluctuations but remain in the upper 30s, suggesting persistent high fire risk conditions, while wet season temperatures are notably lower, staying within the high 20s. Overall, it suggests a trend of decreasing burned area, possibly influenced by climatic variations or improved fire management, despite consistently high dry season temperatures.

**Table 1** Average hot temperature for the given years

Year	2016-2018	2019-2020	2020-2021	2022-2023	2023-2024
fire area calculated (ha)	63.86	53.8	32.7	41.2	33.13
Avg hot temp (dry season) °C	38.9	38.7	38.15	38.64	38.5
Avg hot temp (wet season) °C	28.02	28.95	27.34	27.1	27.5
Annual high temp °C	39.97	39.88	39.16	39.51	39.5

1. Fire area and dry season temperature correlation is ( $r = 0.82$ ); it means that higher temperatures during the dry season led to more extensive fire activity. Fig. 6(a) shows the scattered plot of fire area and dry season temperature.
2. Fire area and wet season hot temperature correlation is ( $r = 0.65$ ); we can assume that the wet season also play small significant role on the burned area fire activity. Fig. 6(b) shows the scattered plot of fire area and wet season temperature.
3. Fire area and annual temperature correlation is ( $r = 0.91$ ); we can assume that the annual temperature of the area has a higher effect on the fire activity. Overall higher temperatures throughout the year have a significant impact on forest fire severity. This suggests that both seasonal and annual temperature increases are important factors in fire risk. Fig. 6(c) shows the scattered plot of fire area and annual temperature.



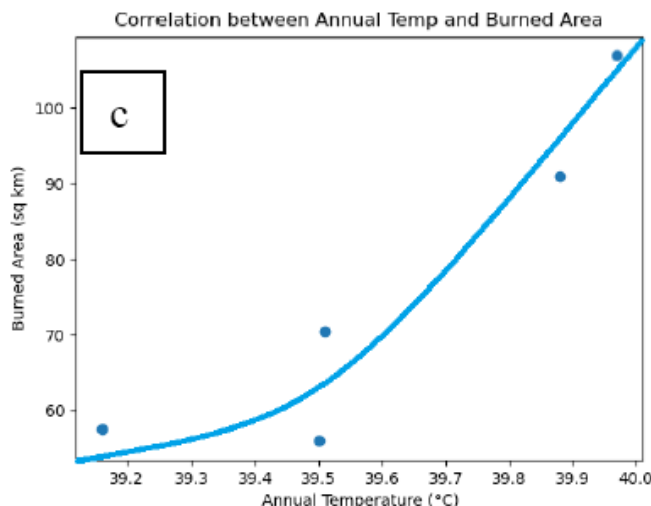


**Fig. 6** Scattered plots of correlation (a) Fire area and dry season temperature. (b) Fire area and wet season temperature. (c) Fire area and annual temperature.

## V. Discussion

### Discussion between LST and dNBR result

The Land Surface Temperature (LST) map provides critical insights into the thermal characteristics of the studied area, revealing spatial temperature variations that are influenced by fire impact and topographic factors. The observed temperature distribution indicates distinct zones, where higher LST values (red or orange areas) correspond to surfaces that absorb and retain heat, while lower LST values (blue or green areas) represent relatively cooler regions.

High LST regions (red or orange): these areas represent burned surfaces, which absorb and retain more heat due to their lower moisture content and lack of vegetation. These regions correspond to highly burned zones, where vegetation loss increases surface temperature.

Low LST regions (blue or green): These areas indicate unburned forest patches or areas with significant vegetation recovery.

Transition zones and intermediate LST (yellow or light orange): represent areas undergoing partial fire damage, mixed land cover, and recent vegetation regrowth. These regions also indicate moderate burn severity, where fire impacted the landscape but did not completely remove vegetation cover.

The spatial pattern of LST can be used to validate burn severity classifications derived from indices like dNBR, helping to distinguish between high-severity burns and areas with partial recovery. Overall, the LST results highlight the thermal heterogeneity of the landscape and provide valuable information for understanding the extent and impact of fire, land cover changes, and post-fire recovery dynamics. Further integration with dNBR and vegetation indices would enhance the accuracy of fire impact assessments.

### Discussion between fire area and seasonal temperature

The results confirm that temperature, particularly during the dry season and across the year, is a key driver of forest fire extent. The data and visualizations provide clear evidence that temperature plays a central role in influencing forest fire dynamics, particularly in terms of the total area burned. In Fig. 6(a), 6(b), and 6(c), the strong positive correlations between annual, wet season, and dry season temperatures and the burned area indicate that higher temperatures contribute to more extensive fire outbreaks. Among these, dry season temperature (Fig. c) demonstrates the most prominent influence. This is consistent with the known fire behavior in tropical and subtropical ecosystems, where hot and dry conditions exacerbate vegetation dryness, reduce fuel moisture, and promote rapid fire spread.

### Conclusion

Based on our analysis of forest fires in the Chagni area from 2016 to 2024, incorporating dNBR, LST and seasonal patterns the following conclusions are made:

To reduce fire risks, prioritize fire prevention strategies during periods of high temperatures, especially during the dry season. Fire risk models should incorporate annual temperature trends to forecast potential fire seasons more accurately.

Integrate LST trends with fire detection models to enhance early warning systems. Using real-time satellite data to track temperature fluctuations and detect potential fire outbreaks. Also, implementing threshold-based alerts combining LST and dNBR values for proactive fire management.

Targeted fire prevention strategies, fire prevention efforts on peak fire months (March–May) when high LST values correlate with severe fire risk. Conduct controlled burns and vegetation management in high-risk zones before the dry season to reduce fuel loads. Strengthen community awareness programs on fire hazards during the dry season. Develop firebreaks and buffer zones in regions where steep slopes and high LST values indicate greater fire vulnerability.

By implementing these strategies, fire management in the Ethiopian highlands can be more proactive and data-driven, ultimately reducing fire severity and improving resilience against wildfire disasters.

### Acknowledgements

This work was supported by the National Natural Science Foundation of China (42307560), the Key Scientific Research Projects of Colleges and Universities in Henan Province (24A170014), the National Undergraduate Training Program for Innovation and Entrepreneurship (202410463021), the High-Level Foreign Expert Recruitment Program of Henan Province (HNGD2025025), the Key Projects of Science and Technology Research of Henan Province (232102320268), the International Science and Technology Collaboration Program of Henan Province (252102520050), and the Cultivation Programme for Young Backbone Teachers in Henan University of Technology (21421292).

### References

- [1] Gitas, I. Z., Mitri, G. H., & Ventura, G. (2012). Object-based image classification for burned area mapping of Creus Cape, Spain, using NOAA-AVHRR imagery. *Remote Sensing of Environment*, 120, 1–9.
- [2] Chuvieco, E., Giglio, L., & Justice, C. (2006). Global characterization of fire activity: Toward defining fire regimes from Earth observation data. *Global Change Biology*, 14(7), 1488–1502.
- [3] Veraverbeke, S., Hook, S. J., & Hulley, G. C. (2014). An alternative spectral index for rapid fire severity assessments. *Remote Sensing of Environment*, 136, 28–35.
- [4] Sun, Y., Zhang, H., & Gong, P. (2019). Improving burn severity estimation using Landsat data by incorporating pre-fire vegetation conditions. *Remote Sensing*, 11(5), 517.
- [5] Miller, J. D., & Thode, A. E. (2009). Quantifying burn severity in a heterogeneous landscape with a relative version of the delta Normalized Burn Ratio (dNBR). *Remote Sensing of Environment*, 109(1), 66–80.
- [6] Bastarika, A., Chuvieco, E., & Martín, M. P. (2011). Mapping burned areas from Landsat TM/ETM+ data with a two-phase algorithm: Balancing omission and commission errors. *Remote Sensing of Environment*, 115(4), 1003–1012.
- [7] U.S. Geological Survey (USGS). (n.d.). Using USGS Landsat Level-1 Data Product. Retrieved from <https://www.usgs.gov/landsat-missions/using-usgs-landsat-level-1-data-product>
- [8] Meng, X., Cheng, J., Zhao, S., Liu, S., & Yao, Y. (2019). Estimating Land Surface Temperature from Landsat-8 Data using the NOAA JPSS Enterprise Algorithm. *Remote Sensing*, 11(2), 155.
- [9] Hexagon Geospatial. (n.d.). Converting Landsat 8 Thermal Band 10 to Temperature Values. Retrieved from [https://supportsi.hexagon.com/s/article/Converting-Landsat-8-Thermal-Band-10-to-Temperature-values?language=en\\_US](https://supportsi.hexagon.com/s/article/Converting-Landsat-8-Thermal-Band-10-to-Temperature-values?language=en_US)
- [10] Esri. (n.d.). Deriving Temperature from Landsat 8 Thermal Bands (TIRS). Retrieved from <https://www.esri.com/arcgis-blog/products/deriving-analytics/deriving-temperature-from-landsat-8-thermal-bands-tirs/>
- [11] Hidalgo-García, D. (2021). Determination of land surface temperature using Landsat 8 images: Comparative study of algorithms on the city of Granada. *Revista de Teledetección*, (57), 1–15.
- [12] Key, C. H., & Benson, N. C. (2006). Landscape assessment: Remote sensing of severity, the Normalized Burn Ratio; and ground measure of severity, the Composite Burn Index.
- [13] Suresh Babu, S. (2018). Estimation of Land Surface Temperature using LANDSAT 8 Data. *International Journal of Advance Research, Ideas and Innovations in Technology*, 4(2).
- [14] Kamila, A., Paul, A. K., & Bandyopadhyay, J. (n.d.). Estimation and Validation of Land Surface Temperature (LST) from Landsat 8 OLI and TIRS sensor's Data. *International Journal of Research*
- [15] Veraverbeke, S., Lhermitte, S., Verstraeten, W. W., & Goossens, R. (2014). The temporal dimension of differenced Normalized Burn Ratio (dNBR) fire/burn severity studies: The case of the large 2007 Peloponnese wildfires in Greece. *Remote Sensing of Environment*, 114(11), 2548–2563.
- [16] Weng, Q., Lu, D., & Schubring, J. (2004). Estimation of land surface temperature–vegetation abundance relationship for urban heat island studies. *Remote Sensing of Environment*, 89(4), 467–483.
- [17] Sobrino, J. A., Jiménez-Muñoz, J. C., & Paolini, L. (2004). Land surface temperature retrieval from LANDSAT TM 5. *Remote Sensing of Environment*, 90(4), 434–440.
- [18] Jiménez-Muñoz, J. C., & Sobrino, J. A. (2003). A generalized single-channel method for retrieving land surface temperature from remote sensing data. *Journal of Geophysical Research: Atmospheres*, 108(D22).
- [19] Wan, Z., & Dozier, J. (1996). A generalized split-window algorithm for retrieving land-surface temperature from space. *IEEE Transactions on Geoscience and Remote Sensing*, 34(4), 892–905.
- [20] Li, Z. L., Tang, B. H., Wu, H., Ren, H., Yan, G., Wan, Z., ... & Zhou, C. (2013). Satellite-derived land surface temperature: Current status and perspectives. *Remote Sensing of Environment*, 131, 14–37.